Correspondence to:
J. Hopkins,
jhopkins@bigelow.org

Phenological characteristics of global coccolithophore blooms

Jason Hopkins[1,2], Stephanie A. Henson[3], Stuart C. Painter[3], Toby Tyrrell[1], and Alex J. Poulton[3]

[1]School of Ocean and Earth Science, National Oceanography Centre Southampton, University of Southampton, Southampton, UK, [2]Now at Bigelow Laboratory for Ocean Sciences, East Boothbay, Maine, USA, [3]Ocean Biogeochemistry and Ecosystems, National Oceanography Centre Southampton, Southampton, UK

Abstract Coccolithophores are recognized as having a significant influence on the global carbon cycle through the production and export of calcium carbonate (often referred to as particulate inorganic carbon or PIC). Using remotely sensed PIC and chlorophyll data, we investigate the seasonal dynamics of coccolithophores relative to a mixed phytoplankton community. Seasonal variability in PIC, here considered to indicate changes in coccolithophore biomass, is identified across much of the global ocean. Blooms, which typically start in February–March in the low-latitude (~30°) Northern Hemisphere and last for ~6–7 months, get progressively later (April–May) and shorter (3–4 months) moving poleward. A similar pattern is observed in the Southern Hemisphere, where blooms that generally begin around August–September in the lower latitudes and which last for ~8 months get later and shorter with increasing latitude. It has previously been considered that phytoplankton blooms consist of a sequential succession of blooms of individual phytoplankton types. Comparison of PIC and chlorophyll peak dates suggests instead that in many open ocean regions, blooms of coccolithophores and other phytoplankton can co-occur, conflicting with the traditional view of species succession that is thought to take place in temperate regions such as the North Atlantic.

1. Introduction

Phytoplankton blooms are associated with periods when environmental conditions promote a rapid growth of phytoplankton stock that outstrips losses from mortality and grazing [*Miller*, 2004]. As the bloom develops, community structure is traditionally thought to transform over time, as changes in environmental conditions and the availability of nutrients favor the survival of one taxon over another, leading to a succession of phytoplankton functional types [*Margalef*, 1978]. This fundamental theory describing changes in community structure (encapsulated in Margalef's mandala) is based on differences in the abilities of competing taxa to survive as nutrient and turbulence conditions change. In the Maraglef mandala [*Margalef*, 1978], phytoplankton taxa are distributed along an axis from diatoms, associated with high-turbulence and high-nutrient conditions, to dinoflagellates, associated with low-turbulence and low-nutrient conditions, with coccolithophores proposed to occupy an ecological niche between these two extremes [*Margalef*, 1978; *Balch*, 2004]. According to this view, continuously changing environmental conditions lead to a succession in taxa, with each taxon replacing its predecessor, as it is better adapted to survive in the modified environment.

Contrary to this idea of sequential changes in phytoplankton taxa, observations of nondiatom and diatom populations co-occurring suggest that coexistence between phytoplankton taxa is also possible [*Barber and Hiscock*, 2006]. This alternative view suggests that instead of undergoing succession, diatoms and nondiatoms may grow contemporaneously, with relative changes in biomass leading to one taxon coexisting with the other. Here we examine the possibility of coexistence between coccolithophores and other phytoplankton.

Blooms of noncalcifying phytoplankton have previously been studied using remotely sensed chlorophyll data to investigate seasonal variability [e.g., *Yoder et al.*, 1993], interannual variability [e.g., *Henson et al.*, 2009], phenology [e.g., *Siegel et al.*, 2002], and phenological variability [*Racault et al.*, 2012]. Phenological indices, such as bloom start date, peak concentration, peak date, and bloom duration can be used to compare blooms on both regional and global scales, while seasonal and interannual variability in these indices can provide insights into potential influences on bloom initiation such as the interplay between mixed-layer depth and light [*Zhai et al.*, 2011], the breakdown in turbulent mixing, and changes in net heat flux [*Taylor and Ferrari*, 2011; *Brody et al.*, 2013; *Smyth et al.*, 2014] and changes in wind stress [*González Taboada and Anadón*, 2014]. Observations of chlorophyll data alone, however, provide little information about changes in community structure.

Coccolithophores are a key phytoplankton group that have a major influence on the marine carbon cycle, particularly the inorganic carbon pump [*Broecker and Clark*, 2009] and often represent 5–40% of primary production [*Poulton et al.*, 2007, 2013]. These single-celled algae produce an external coccosphere composed of individual calcium carbonate plates (coccoliths) [*Paasche*, 2002] which are a major contributor to the global export flux of calcium carbonate [*Milliman*, 1993; *Broecker and Clark*, 2009]. The process of pelagic calcite production is biogeochemically important in that it can influence both the magnitude of the air-sea gradient of CO_2, weakening CO_2 sinks caused by photosynthesis [*Harlay et al.*, 2010; *Shutler et al.*, 2013], and the efficiency of the transport of organic detrital matter through the water column by means of a "ballasting" effect [e.g., *Klaas and Archer*, 2002], although the impact of this has recently been questioned [*Henson et al.*, 2012]. In addition, coccolithophores may well be sensitive to changes in ocean pH [e.g., *Doney et al.*, 2009] and might therefore be a crucial indicator of the impact of climate change in the marine environment.

Coccolithophores have been identified in the majority of the world's oceans [e.g., *Brown and Yoder*, 1994; *Winter et al.*, 1994; *Iglesias-Rodríguez et al.*, 2002], and their coccoliths are recognized as being a major source of backscattering of light from the ocean [*Balch et al.*, 1991]. During the rapid growth conditions of a bloom some species of coccolithophore (e.g., *Emiliania huxleyi*) can overproduce and shed excess coccoliths into the surrounding water column [*Paasche*, 2002], creating vast patches ($>250,000 \, km^2$ [*Holligan et al.*, 1993a]) of calcium carbonate in the surface ocean, most notably in the temperate latitudes [*Tyrrell and Merico*, 2004]. It is the characteristic light scattering properties of coccoliths that enables coccolithophore blooms to be observed in satellite ocean color data [e.g., *Holligan et al.*, 1983; *Brown and Yoder*, 1994; *Iglesias-Rodríguez et al.*, 2002; *Balch et al.*, 2005]. Early work using satellite data provided considerable insights into the global distribution and spatial extent of coccolithophore blooms [*Brown and Yoder*, 1994; *Iglesias-Rodríguez et al.*, 2002]; however, our understanding of how these blooms develop over time tends to be limited to regional rather than global studies [e.g., *Brown and Yoder*, 1994; *Signorini and McClain*, 2009; *Shutler et al.*, 2010; *Poulton et al.*, 2013; *Balch et al.*, 2014].

The common bloom-forming coccolithophore, *Emiliania huxleyi*, has a small cell size ($< 5 \, \mu m$) [*Paasche*, 2002] and forms blooms that typically have low chlorophyll concentrations ($<2 \, mg \, chl \, a \, m^{-3}$ [*Holligan et al.*, 1993b]) because, although such blooms contain relatively high numbers of cells, each *E. huxleyi* cell contains only a very small amount of chlorophyll a ($< 0.4 \, pg$ [e.g., *Daniels et al.*, 2014]). Blooms of coccolithophores such as *E. huxleyi* are therefore likely to make only a small contribution to the chlorophyll signal that is traditionally used to chart the seasonal progression of phytoplankton biomass.

The NASA Ocean Color chlorophyll product is determined from ratios of remote sensing reflectance in the blue and green wavelengths, and the current Moderate Resolution Imaging Spectroradiometer (MODIS) Ocean Color chlorophyll algorithm (OC3M) uses three bands (443, 489, and 547 nm) in one of the two possible ratios to derive estimates of chlorophyll concentration. Similar to previous studies [e.g., *Siegel et al.*, 2002; *Henson et al.*, 2009; *Racault et al.*, 2012], this analysis uses a threshold method to determine key phenological indices such as bloom initiation date, peak date, and duration; however, unlike these prior studies, we use remotely sensed PIC data to determine the global phenological characteristics of just blooms of coccolithophores.

Coccoliths tend to scatter rather than absorb light entering the ocean [*Balch et al.*, 1996], and a robust relationship between the amount of backscattered light and coccolith concentration provides the means to estimate upper ocean PIC concentration [*Balch et al.*, 2005]. The MODIS PIC product is derived from a merged algorithm [*Gordon et al.*, 2001; *Balch et al.*, 2005]. The two-band method [*Balch et al.*, 2005], based upon the semianalytical model of ocean color developed by *Gordon et al.* [1988], uses a look-up table of measurements of normalized water leaving radiance at two wavelengths (443 and 555 nm) to determine PIC concentrations. If this method fails to obtain a retrieval, for example, if reflectance values fall outside of the bounds of the look-up table, then the algorithm switches to the three-band method derived by *Gordon et al.* [2001], which uses spectral bands in the red and near-infrared (670, 765, and 865 nm) to determine coccolithophore calcite concentration. The MODIS PIC product has been successfully validated in a number of locations using shipboard reflectance measurements, underway measurements of acid labile backscatter, and in situ measurements of PIC concentration [e.g., *Balch et al.*, 2005, 2009, 2011].

Although other particulate matter within the water column may also contribute to the backscattered light field, we consider that (a) the cosmopolitan nature of coccolithophores, in particular *E. huxleyi* [*Winter et al.*, 1994;

(b) observations that *E. huxleyi* forms widespread blooms [e.g., *Holligan et al.*, 1993a] and is perhaps unique in that it sheds huge numbers of coccoliths into the water column [*Paasche*, 2002]; plus (c) evidence that the optical backscattering cross section of calcite particles the size *E. huxleyi* coccoliths is orders of magnitude greater than other calcite particles [*Balch et al.*, 2005] mean that seasonal variability in PIC concentration is most likely driven by changes in coccolithophore abundance.

The study of phytoplankton phenology has historically been undertaken using satellite chlorophyll data and has tended to have been biased toward the Northern Hemisphere spring bloom [*Ji et al.*, 2010]. The use of remotely sensed PIC concentration data offers a unique opportunity to compare the seasonal cycle of coccolithophores separate to that of the noncalcifying phytoplankton population and to evaluate the evidence for phytoplankton population succession [*Margalef*, 1978] or coexistence [*Barber and Hiscock*, 2006] on a global scale.

2. Methods

2.1. Satellite Data

AQUA MODIS 9 km resolution, 8 day composite PIC, and chlorophyll products (R2012.0 reprocessing) from July 2002 to December 2012 were downloaded from the NASA Ocean Color website (http://oceancolor.gsfc.nasa.gov). The use of 8 day composite data offered a trade-off between minimizing data gaps (combining several overpasses reduces the effect of interorbital gaps and cloud cover) while maintaining a suitable temporal resolution for capturing bloom timing.

The data sets were spatially regridded to 1° resolution to reduce noise in the data and further improve spatial data coverage. In the Northern Hemisphere, a year was defined as January to December and data from January 2003 to December 2012 were used to construct a 10 year time series. In the Southern Hemisphere a year was defined as July to June to account for the seasonal offset and data from July 2002 to June 2012 were used to produce the 10 year time series. Interannual variability was calculated as the standard deviation of 10 years of phenological metric data.

2.2. Data Selection

A climatological time series was created for each pixel of data, representing the 10 year average seasonal cycle. This was assessed to identify whether a pixel possessed a pronounced seasonal cycle and to evaluate the proportion of missing data caused, for example, by cloud cover or low Sun angle in winter. Time series with a coefficient of variation (standard deviation/mean) in the PIC or chlorophyll data of ≤0.35 [*Cole et al.*, 2012] or those pixels with > 240 days of missing data (chosen as a suitable cutoff through a comprehensive visual examination of the time series) were excluded from further analysis. Data from an area of the South Pacific gyre where PIC concentrations are low and highly variable were also excluded due to a lack of confidence in the robustness of any phenological information derived from such data with an exceptionally low signal-to-noise ratio. This region of the South Pacific gyre has previously been associated with anomalous measurements of satellite-derived chlorophyll, possibly caused by exceptionally clear waters enhancing the optical effects of particulate matter within the water column [*Claustre and Maritorena*, 2003].

The exclusion of regions with low variability and/or time series with relatively large amounts of missing data meant that our analysis was confined to between latitudes of 30° and 70° in both hemispheres but included some regions of the equatorial Atlantic and Arabian Sea.

2.3. Phenological Metrics

A novel algorithm was developed to estimate key phenological characteristics from the annual and climatological time series of PIC and chlorophyll data. The algorithm first filled any short gaps (< 4 satellite time steps, most likely caused by cloud cover) through linear interpolation between adjacent data points in the time series. Linear interpolation was employed in preference to the use of climatological values to fill gaps on the basis that the substitution of data points could have resulted in perturbations in the time series that were not necessarily representative of the prevailing PIC concentrations at that time.

Next, bloom conditions were defined for each time series. There are a number of indices [*Ji et al.*, 2010] and methods [*Brody et al.*, 2013] that can be used in the determination of key bloom timings. *Brody et al.* [2013] compared a threshold method, a rate of change method, and a cumulative method and found that each had
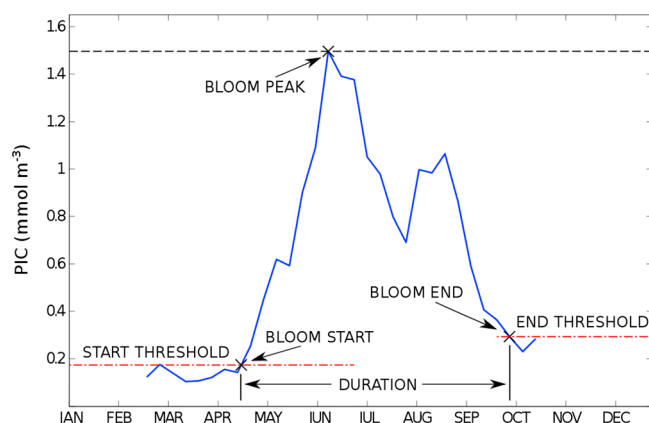
Figure 1. Example of phenology metric identification. Red dotted line indicates the start and end thresholds (prepeak or postpeak minimum plus 5% of prepeak or postpeak range). Crosses indicate key phenological characteristics determined from the algorithm.

its own strengths and weaknesses. Similarly, *Ji et al.* [2010] reviewed different indices that had been used in phytoplankton phenology studies, finding that the most appropriate metric depended on the investigation being undertaken, the location, and the forcing mechanism involved.

There is no common consensus as to what constitutes a bloom [*Smayda*, 1997]. Although traditionally considered to be a period of significant biomass increase, we use the term "bloom" in a more wide-ranging sense to represent the period that PIC concentration remains above a defined threshold. As such, our definition of a bloom encompassed periods of both PIC increase and decline within the entire seasonal cycle of PIC concentration. Often it is common for a static threshold definition, based on cell numbers [e.g., *Tyrrell and Taylor*, 1996], to be used when defining coccolithophore blooms. While this might be considered a valid metric for regional studies, variability in environmental carrying capacity may lead to spatial inconsistencies in maximum achievable cell densities on a global scale [*Smayda*, 1997]. We therefore selected a dynamic threshold, more appropriate for a global study such as this that encompasses many different oceanographic regimes.

Brody et al. [2013] concluded that blooms with a longer duration resulted in an elevated annual median and, as a consequence, had later start dates. When comparing the initiation dates of blooms, it is important to reduce any potential bias that a difference in bloom shape might have on the determination of the start date of the bloom. Therefore, we have adapted the commonly used threshold method [e.g., *Siegel et al.*, 2002; *Henson et al.*, 2009; *Racault et al.*, 2012] but removed the reliance on the annual median as the basis for the bloom threshold, eliminating the impact that different bloom shapes might have in determining the timing of initiation.

Our method, which is applied to both PIC and chlorophyll satellite data, used the annual maximum (peak) concentration to divide each year of data into a prepeak and a postpeak period. The bloom start threshold was defined as the prepeak minimum concentration plus 5% of the range between the prepeak minimum and peak concentration, while the bloom end threshold was defined as the postpeak minimum concentration plus 5% of the range between the peak and postpeak minimum concentration (illustrated in Figure 1). The algorithm then worked backward in time from the peak of the bloom to identify the first two consecutive data points below the start threshold. The bloom start date was determined by interpolation between the data points above and below the start threshold. The bloom end date was determined in a similar manner by moving forward in time from the bloom peak and with reference to the bloom end threshold. The duration of the bloom, which corresponded to the period that PIC remains above our defined bloom thresholds, was determined from the difference between bloom start and bloom end dates. The peak date was defined as the time of maximum concentration. The results were subsequently converted to, and presented as, monthly intervals for visualization of the large-scale pattern in phenology.

2.4. Regional Analyses

Six areas were selected to compare and contrast the regional variability in PIC and chlorophyll concentrations (see Figures 2–5 for locations). These areas were selected based on literature observations of in situ coccolithophore blooms as well as for their contrasting oceanographic conditions. The algorithm was applied to 5° × 5° spatially binned PIC and chlorophyll data from the North Pacific (48–53°N, 142–147°W), an area of the North Atlantic (Iceland Basin; 57–62°N, 17–22°W), and part of the Barents Sea (72–77°N, 32–37°E). In the Southern Hemisphere we used data from the South Pacific (55–60°S, 90–95°W), an area adjacent to the Patagonian Shelf (47–52°S, 58–63°W), and a region to the north of South Georgia (48–53°S, 35–40°W) to

produce regional time series. The seasonal cycles for each box were derived from the climatological average of 10 years of data.

2.5. Identifying Succession or Coexistence

We defined succession or coexistence characteristics through the relative timing of the peaks in the climatological seasonal cycles of chlorophyll and PIC data. The signature of phytoplankton succession was characterized as a substantial lag (>24 days) between the peak in chlorophyll and the peak in PIC concentration, while coexistence between populations was defined as peaks in the two variables that occurred within ±16 days of each other (±2 satellite time periods being considered to be a sufficiently small interval relative to the temporal resolution to represent coexistence). These criteria were applied to each separate year of the 10 years of available data, and the number of occurrences of either criterion in each pixel was determined. These were then used to calculate the percentage likelihood of each pixel exhibiting succession or coexistence characteristics. Only pixels that demonstrated a clear indication of either succession or coexistence (> 60% likelihood) are presented.

2.6. Limitations of the Data

Analyses based on satellite-derived data have their limitations. First, satellite data from regions close to the coast (Case II waters) are notoriously difficult to interpret due to the influence that abiogenic particulate matter can have on measurements of ocean color [*Morel and Prieur*, 1977]. We have confined the majority of our observations to relatively deep (Case I) waters using a 150 m bathymetric mask. Second, we recognize the problems that resuspended material can create for reliable estimates of coccolithophore abundance via PIC concentration [*Broerse et al.*, 2003; *Weeks et al.*, 2004; *Daniels et al.*, 2012] and so adopt a similar approach to that taken above, confining our observations mainly to the open ocean, away from shallow (< 150 m deep) water. Third, the determination of the phenological characteristics of blooms using satellite data is not completely objective, being influenced not only by the method used but also by the definition used to describe bloom/nonbloom conditions. When *Brody et al.* [2013] compared three different methods for determining bloom initiation in the North Atlantic, they found that each method produced different patterns in bloom initiation. In addition, the choice of index studied will depend on (a) the characteristic of the bloom that is under investigation and (b) the advantages and disadvantages associated with that particular index [*Ji et al.*, 2010]. Missing data have also been identified as a limitation in efforts to determine phenological indices using satellite data [*Cole et al.*, 2012; *Brody et al.*, 2013; *Racault et al.*, 2014]. We have attempted to mitigate the impact of missing data through the use of climatological time series where appropriate and the filling of small gaps (< 4 satellite time periods) by linear interpolation between data points in a time series. Fourth, high concentrations of coccoliths may remain after cell populations begin to decline [*Tyrrell and Merico*, 2004; *Young et al.*, 2014]. Therefore, while we consider that remotely sensed PIC concentration data can reasonably be used as a proxy for coccolithophore abundance up to the peak of the bloom, the change in cell to coccolith ratio after this point in the development of a bloom may lead to a decoupling of the relationship between the organic (cell) and inorganic (coccolith) fractions. After the peak, PIC may therefore become less reliable as a proxy for coccolithophore abundance. While calcite particles the size of an *E. huxleyi* coccolith are by far the major contributor to backscatter at 546 nm [*Balch et al.*, 1996], we recognize that relative contribution to backscatter by other constituents in the water column may change, particularly at low PIC concentrations. This background PIC level provides a baseline and any rise above this level we consider to be driven by an increase in the coccolithophore population. Finally, as with all analyses using satellite data, interpretation is limited to retrievals over the first optical depth and therefore excludes the influence of deeper patterns of biomass.

3. Results

3.1. Coccolithophore Bloom Phenology

In the Northern Hemisphere PIC concentration starts to increase, and hence, the annual coccolithophore bloom begins, between January and July, while in the Southern Hemisphere the bloom starts between June and December (Figure 2a). Broad latitudinal patterns are seen in both hemispheres with a progressive delay in bloom start date from low to high latitudes. This pattern is particularly evident in the North Atlantic where the bloom starts in March at ~ 40°N but is delayed until May at ~ 60°N. While blooms tend to start between February and May in the North Pacific, unlike the North Atlantic, there is no latitudinal progression. The
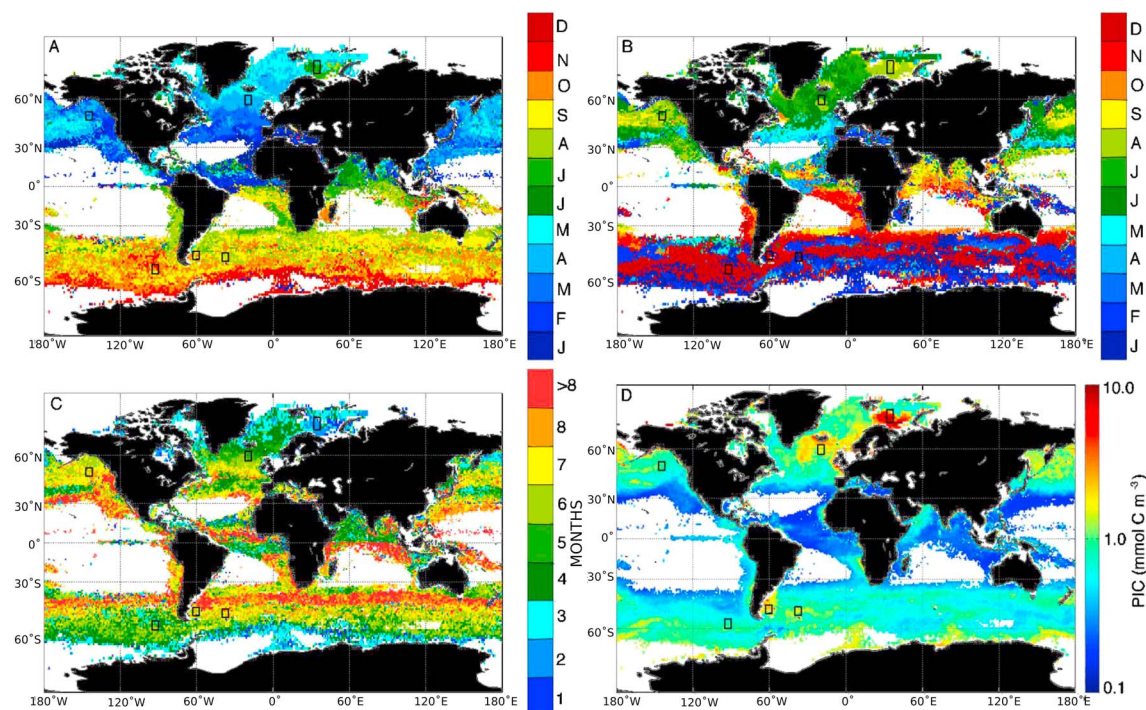
Figure 2. Coccolithophore bloom phenology: (a) bloom start month, (b) bloom peak month, (c) bloom duration, and (d) peak PIC concentration. Black squares indicate regions of interest. White areas represent regions with low variability, persistent periods of missing data, or water column depth <150 m. Metrics calculated from 10 year climatological average.

Barents Sea is characterized by later bloom start dates (July), relative to those observed in the rest of the Northern Hemisphere. While the pattern in the data in the Southern Hemisphere is patchier than that in the Northern Hemisphere, there is evidence of a similar, but less distinct, latitudinal progression in bloom start date (August–December) across the majority of the Southern Ocean, with the exception of the region associated with the sub-Antarctic South Pacific (Figure 2a).

The peak date in the annual PIC cycle is shown in Figure 2b. The Northern Hemisphere is generally characterized by peak dates that occur between June and September, although there is evidence of earlier peak dates (March–April) in the midlatitudes (~30°–40°N) of the North Atlantic and North Pacific. The Southern Hemisphere is dominated by a sub-Antarctic band of peak dates that occur between December and February. There is also evidence of earlier peak dates (September–October) at lower latitudes (~30°S) in the South Atlantic.

In general, blooms are shorter but more intense moving from low (~30°) to high (~70°) latitudes: reducing from ~6–7 months to 2–3 months in the Northern Hemisphere and from ~9 months to 2–3 months in the Southern Hemisphere (Figure 2c). This latitudinal progression appears patchier in the northern sector of the Pacific compared to elsewhere. In the Northern Hemisphere, blooms with the longest duration (~9 months) are associated with the edge of the subtropical convergence zone (~30°N), while the shortest (~2 months) are observed in the Barents Sea. In the Southern Hemisphere, a band of relatively long duration blooms (8–9 months) is associated with the ~40°S parallel, while the shortest duration blooms are found within the South Atlantic portion of the Antarctic Circle (~60°S).

The spatial variability in the intensity of coccolithophore blooms is assessed from the maximum (peak) annual PIC concentration and is shown in Figure 2d. The lowest peak PIC concentrations (~0.1 mmol C m^{-3}) tend to be associated with the low latitudes (10°N and 10°S) and the outer edges of the major ocean basin gyres. Peak PIC concentrations generally increase from ~0.1 mmol C m^{-3} to ~1 mmol C m^{-3} moving poleward in both hemispheres. There is evidence of discrete high-magnitude (>1 mmol C m^{-3}) patches of PIC in the Irminger Basin, Norwegian Sea, and the Barents Sea in the Northern Hemisphere and along the Patagonian Shelf in the
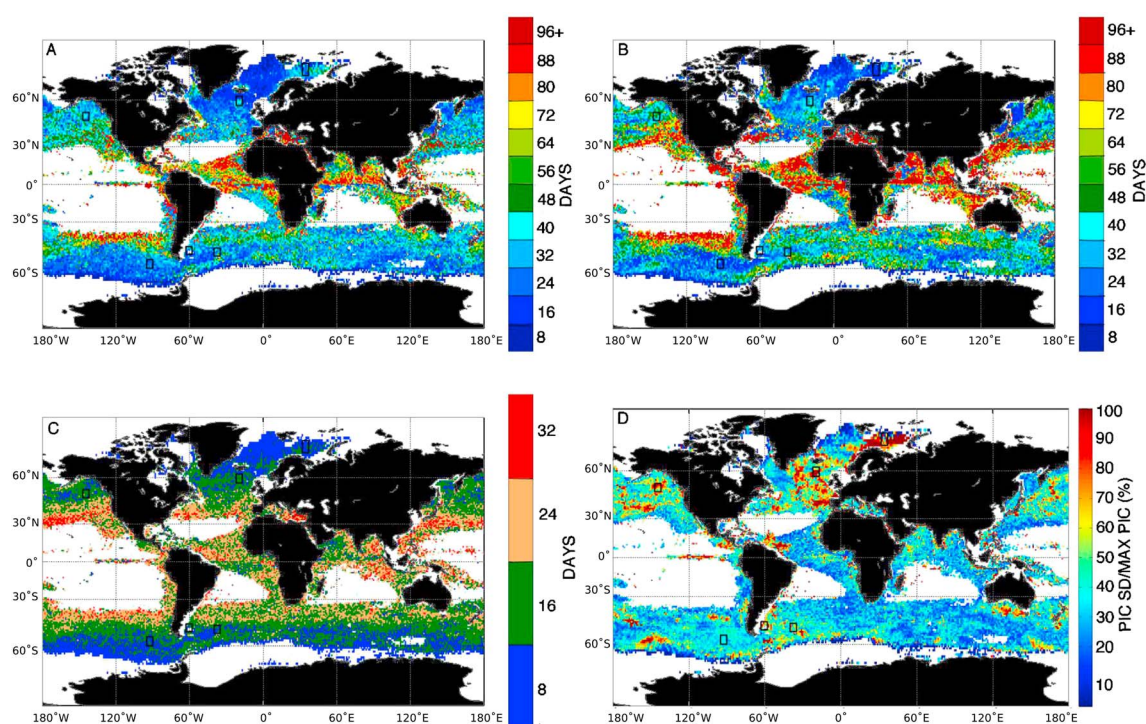
HOPKINS ET AL.   244

Figure 3. Interannual variability in coccolithophore bloom phenology from 2003 to 2012: (a) start date, (b) peak date, (c) duration, and (d) peak PIC concentration. Black squares indicate regions of interest. White areas represent regions with low variability, persistent periods of missing data, or water column depth <150 m.

Southern Hemisphere. These are all regions associated with intense blooms of the coccolithophore *Emiliania huxleyi*, as documented by numerous in situ observations [e.g., *Holligan et al.*, 1993a; *Smyth et al.*, 2004; *Poulton et al.*, 2013].

3.2. Interannual Variability in Coccolithophore Blooms

Interannual variability in the phenological characteristics is presented in Figure 3. Global variability in coccolithophore bloom start date (Figure 3a) is relatively low (8–24 days) across a large proportion of the North Atlantic, with the exception of small patches of high variability (32–40 days) in the Iceland Basin, Barents Sea, and lower latitudes. The variability in start date in the North Pacific is 32–48 days and thus higher than that observed in the North Atlantic. Interannual variability in start date across the Southern Hemisphere is 32–48 days and thus broadly similar to that observed in the North Pacific. An exception is the higher-latitude (>50°S) region of the South Pacific where variability in start date (8–32 days) was more comparable to that observed in the North Atlantic. In general, the lowest variability in start date (8–40 days) is associated with higher-latitude regions (~ 60°N and 60°S) while highest variability tends to be associated with the edges of the subtropical gyres and equatorial regions.

Interannual variability in bloom peak date (Figure 3b) exhibits a similar pattern to that seen in coccolithophore bloom start date. In the North Atlantic, variability in peak date is relatively low (8–40 days) compared to the other major basins, with the lowest variability confined to higher latitudes (> 60°N). The North Pacific is associated with higher variability (~32–48 days) in peak date compared to the North Atlantic. In particular, high variability is noted along, and extending out from, the Californian coast (>64 days). The Southern Hemisphere generally exhibits high variability in peak date (~32–64 days) over large spatial areas compared to the Northern Hemisphere. The sub-Antarctic sector of the South Pacific is the exception to this general pattern as it contains large areas where the variability in peak date is lower (8–24 days). In summary, and similar to the pattern observed in the interannual variability in start date, the highest variability in peak date is associated with the edges of the subtropical gyres and equatorial regions.

The variability in bloom duration (Figure 3c) is considerably lower than that observed in either start date or peak date (maximum 32 days). The pattern of interannual variability in this phenological index tends to follow

a relatively well-defined latitudinal progression moving poleward in both hemispheres. The variability in duration is relatively high (~16–32 days) in the midlatitudes (~30°–40°) and gets progressively shorter (~8 days) at higher latitudes (>60°N and 60°S). While highest variability is again associated with the edges of the subtropical gyres and equatorial regions, the overall spatial pattern in duration variability is dominated by strong latitudinal influences. The low range of variability in duration suggests that shifts in start date may be matched by shifts of a similar magnitude in the end date, i.e., an earlier start date is associated with an earlier end date, resulting in low interannual variability in duration.

The interannual variability in peak PIC concentration is presented as the standard deviation of 10 years of peak PIC concentration normalized to the climatological mean peak PIC concentration at that pixel (Figure 3d). This provides an indication of how the magnitude of the coccolithophore blooms varies year to year relative to the average peak concentration. The North Atlantic exhibits patches of high interannual variability (80–100% of the mean peak concentration) in peak concentration interspersed with areas of lower variability (<50%). The highest variability in this region is associated with the Iceland and Irminger basins and off the western Iberian coast. The North Pacific contains similar patches of high variability; however, the spatial distribution of these is much sparser than that observed in the North Atlantic. Peak PIC concentration in the Southern Hemisphere is generally lower than that observed across the Northern Hemisphere (~20–60%). There is evidence of some patches of relatively high variability (70–100%) in the sub-Antarctic South Pacific, to the east of South Georgia, and to the south of Australia; however, the spatial distribution is much patchier than observed in the Northern Hemisphere. Globally, the highest variability is associated with a large area of the Barents Sea (>100%).

3.3. Regional Analysis of Coccolithophore Blooms

The seasonal development of coccolithophore blooms at different geographical locations, assessed from spatially averaged climatological PIC data from six 5° × 5° boxes, is presented in Figure 4. The climatological phenological characteristics for each region are also summarized in Table 1.

In our North Atlantic region, the coccolithophore bloom is characterized by a rapid increase in PIC concentration that begins in spring and rises to an initial peak in early summer. PIC concentration then decreases before increasing again to a lower secondary peak in late summer/early autumn before eventually declining to a minimum in winter (Figure 4). The maximum average PIC concentration in this region is ~1.3 mmol C m^{-3} and the bloom persists on average for ~6 months (Table 1).

The North Pacific regional coccolithophore bloom starts slightly earlier in the spring (March) and increases at a relatively slower rate compared to that of the North Atlantic (Figure 4). It reaches a single peak in the summer/early autumn (August/September). The maximum PIC concentration of this bloom is ~0.8 mmol C m^{-3} (Table 1), with the slower rate of change in PIC concentration resulting in a bloom with a later peak and slightly longer duration (~8 months) than that observed in the North Atlantic.

In contrast, the bloom from the Barents Sea region starts later in the year (June/July) than other blooms in the Northern Hemisphere and is characterized by a single high-magnitude peak in August, which declines rapidly thereafter (Figure 4). Analysis of this short lived, high-magnitude bloom is hampered to some extent by the reduced satellite coverage in this region caused by low Sun angle in winter at high latitudes; however, the available data indicate that the Barents Sea is a region of relatively short lived (~2 months), high-intensity (~4 mmol C m^{-3}) coccolithophore blooms compared to other regions in our study (Table 1).

The selected regions of the Southern Hemisphere are characterized by PIC patterns that are generally similar to those observed in the Northern Hemisphere. The coccolithophore bloom from the region adjacent to the Patagonian Shelf starts in the austral spring (September) and rises to a single peak in late austral summer (December/early January), before declining to a minimum in the austral winter (May; Figure 4). While the magnitude of this bloom (~1.5 mmol C m^{-3}) is similar to the North Atlantic bloom (~1.3 mmol C m^{-3}), it persists for slightly longer (~8 months versus 6 months; Table 1)

The coccolithophore bloom north of South Georgia starts relatively early in the austral spring (August) compared to the Patagonian Shelf break bloom (Figure 4). It rises slowly to a peak late in the austral summer (January/February) with a maximum PIC concentration of ~1.3 mmol C m^{-3} and persists for approximately 8 months (Table 1). The bloom in the sub-Antarctic region of the South Pacific starts in the austral spring
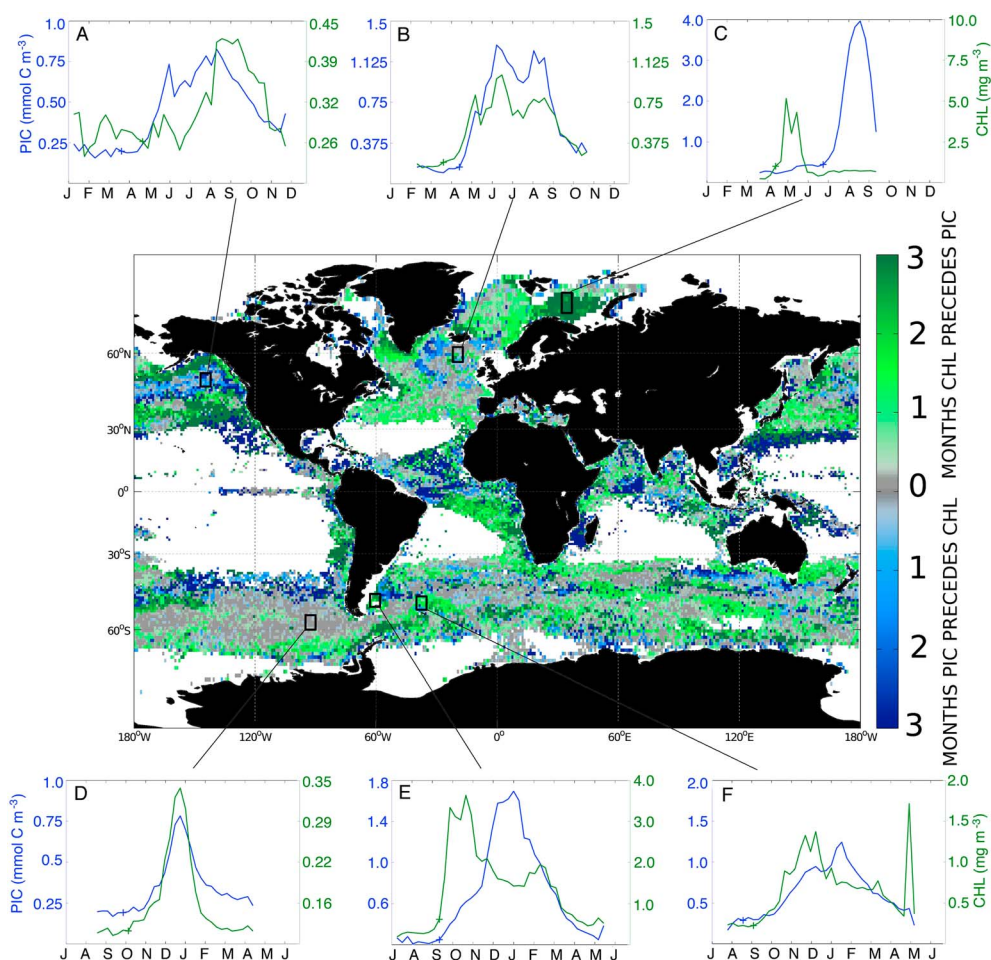
Figure 4. Difference in month of peak date between PIC and chlorophyll (blue = PIC peak precedes chlorophyll peak and green = chlorophyll peak precedes PIC peak). Subplots show climatological time series from (a) North Pacific, (b) North Atlantic, (c) Barents Sea, (d) South Pacific, (e) adjacent to Patagonian Shelf, and (f) north of South Georgia (blue = PIC and green = chlorophyll). Crosses indicate start dates. Note the different scales on Y axes.

(September), rises relatively rapidly to a single peak in the austral summer (December/January), and then declines sharply. This single peak bloom has a shorter duration (~6 months) and lower maximum concentration (~0.8 mmol C m^{-3}) than those blooms from the regions closer to the Patagonian Shelf and to the north of South Georgia (Table 1).

3.4. Comparison of Chlorophyll and PIC Bloom Patterns

The opposing theories of succession [*Margalef*, 1978] and coexistence [*Barber and Hiscock*, 2006] of taxa within the seasonal cycle of phytoplankton are investigated by comparing the timing of maximum PIC

Table 1. Summary of the Key Regional Phenological Characteristics of Coccolithophore Blooms[a]

Region	Start Date of Bloom		Peak Date of Bloom		Duration of Bloom		Maximum PIC Concentration	
	Day	SD	Day	SD	Days	SD	PIC (mmol C m^{-3})	SD (mmol C m^{-3})
North Atlantic	112 (April)	±5 days	156 (June)	±30 days	164	±21 days	1.3	±1.3
North Pacific	85 (March)	±25 days	242 (August)	±34 days	219	±31 days	0.8	±0.7
Barents Sea	183 (July)	±28 days	239 (August)	±6 days	74	±21 days	4.1	±4.0
Patagonian Shelf	265 (September)	±16 days	1 (January)	±13 days	215	±31 days	1.5	±1.1
South Georgia	241 (August)	±22 days	29 (January)	±13 days	237	±30 days	1.3	±0.7
South Pacific	271 (September)	±23 days	2 (January)	±10 days	162	±22 days	0.8	±0.3

[a]Data are derived from the mean and standard deviation of the climatological phenological characteristics from regions of interests.
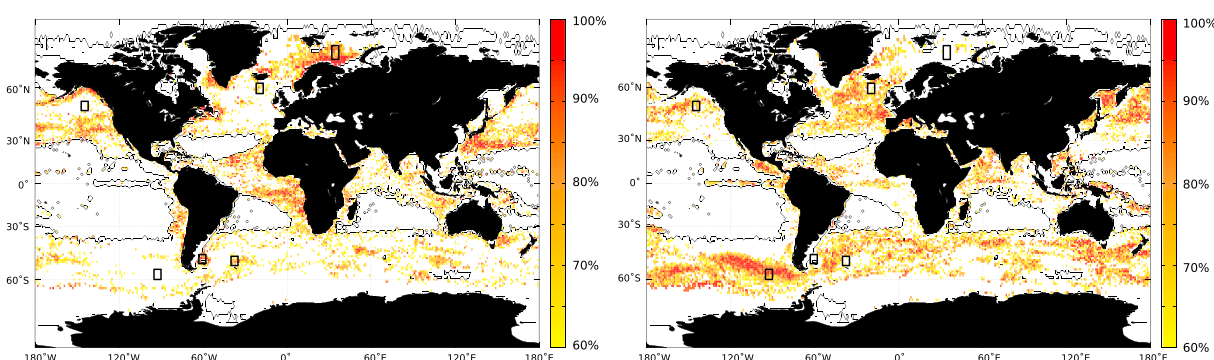
Figure 5. (left) Pixels with >60% likelihood of chlorophyll peak occurring > 32 days before the PIC peak (succession of phytoplankton populations) in 10 years of data. (right) Pixels with >60% likelihood of PIC and chlorophyll peaks occurring within ±16 days of each other (coexistence of phytoplankton populations) in 10 years of data. Black contour lines bound areas with low variability, persistent periods of missing data, or water column depth < 150 m.

concentration with the timing of maximum chlorophyll concentration (Figure 4). While there are large parts of the global ocean where the timing of the peak in chlorophyll precedes the peak in PIC concentration, which might be expected if larger phytoplankton (e.g., diatoms) precede coccolithophores in a pattern of seasonal succession, there are also extensive regions (~46% of the data), particularly in the Southern Ocean and sub-Arctic North Pacific, where the peak in the PIC concentration occurs simultaneously with or precedes the peak in the chlorophyll data (Figure 4).

In the North Atlantic region phytoplankton biomass starts to increase in March, ~1 month before the onset of the coccolithophore bloom; however, both blooms then develop in a similar manner and peak at similar times (chlorophyll mean peak day = 171, temporal standard deviation = 30 days and PIC mean peak day = 156, temporal standard deviation = 24 days), before declining and rising to a lower secondary peak later in the year. In the North Pacific region, our analysis suggests that the coccolithophore bloom starts in March, slightly before the increase in chlorophyll. Both blooms continue to develop at different rates, with the peak in PIC concentration occurring slightly earlier than that observed in the chlorophyll data (chlorophyll mean peak day = 251, temporal standard deviation = 16 days and PIC mean peak day = 242, temporal standard deviation = 34 days). The magnitude of chlorophyll concentration in this region (~0.4 mg m^{-3}) is lower than that observed in the North Atlantic (~1 mg m^{-3}). In the Barents Sea chlorophyll concentration increases to a peak in April and declines again in May, 1 month prior to the start of the coccolithophore bloom (June; Figure 4). In this region, blooms of phytoplankton that dominate the chlorophyll signal appear to be completely decoupled from those of coccolithophores (chlorophyll mean peak day = 134, temporal standard deviation = 13 days and PIC mean peak day = 239, temporal standard deviation = 6 days), reinforcing the point that high PIC can occur in the absence of high chlorophyll.

The start dates of the coccolithophore bloom and the initial rise in chlorophyll in the Southern Hemisphere are closer together than those of the Northern Hemisphere. In the sub-Antarctic South Pacific region, blooms start at slightly different times (late September for PIC and early October for chlorophyll); however, the PIC and chlorophyll data peak at similar times (chlorophyll mean peak day = 1, temporal standard deviation = 9 days and PIC mean peak day = 2, temporal standard deviation = 10 days). Although the PIC and chlorophyll data in the regions adjacent to the Patagonian Shelf and South Georgia start to increase at similar times, the relatively slower rate of change in PIC compared with chlorophyll means that coccolithophore blooms in both regions peak later than chlorophyll concentration. In the region adjacent to the Patagonian Shelf, PIC peaks in January, approximately 3 months after the peak in chlorophyll (chlorophyll mean peak day = 301, temporal standard deviation = 15 days and PIC mean peak day = 1, temporal standard deviation = 13 days), while north of South Georgia maximum PIC concentration occurs in January ~1 month after the peak in chlorophyll (chlorophyll mean peak day = 354, standard deviation = 22 days and PIC mean peak day = 29, standard deviation = 13 days; Figure 4).

The relative timings of the chlorophyll and PIC concentration peaks are used to assess whether blooms of coccolithophores and other noncalcifying phytoplankton co-occur, and thus exhibit some degree of

coexistence between taxa as suggested by *Barber and Hiscock* [2006], or whether coccolithophores peak at different times to other noncalcifying phytoplankton, a scenario more akin to succession of phytoplankton taxa as suggested by *Margalef*'s [1978] mandala. We consider only those pixels that demonstrate an indication of either coexistence or succession characteristics in more than six out of the 10 years of data (Figure 5). Those pixels where succession (i.e., > 24 days difference in the timing of peak dates) occurs in six or more of the 10 years are generally located away from the open ocean or in regions of upwelling, while those pixels where coexistence (i.e., bloom peaks that are within ±16 days of each other) occurs in six or more of the years are primarily associated with open ocean regions.

4. Discussion

4.1. Phenology of Coccolithophore Blooms

We have generated a unique global set of phenological characteristics for coccolithophore blooms using remotely sensed PIC data. While it is difficult to assess the accuracy of our estimates of these key phenological characteristics compared to in situ observations (particularly given the lack of an accepted method to define bloom conditions), our phenological indices are similar to the timings of established coccolithophore blooms. The identification of peak PIC in June in the midlatitude North Atlantic is supported by in situ observations of coccolithophore blooms by *Holligan et al.* [1993a] and *Raitsos et al.* [2006]. In addition, *Schiebel et al.* [2011] observed relatively high *E. huxleyi* cell numbers between 33°N and 47°N in March (corresponding with our estimate of a March peak date in this region), while *Poulton et al.* [2010] report nonbloom conditions in the Iceland Basin in July–August, which match our observations of a decline in PIC concentration from the peak PIC in June. Observations from the Barents Sea [*Smyth et al.*, 2004; *Signorini and McClain*, 2009; *Hovland et al.*, 2013] identify high-reflectance/PIC concentrations in the late summer (July–August), which compares favorably with our observations of an August peak in this region. In addition, our estimates of peak PIC concentrations in December/January along the Patagonian Shelf agree with observations of coccolithophore blooms made by *Signorini et al.* [2006] (January peak) and the timings of high coccolithophore cell numbers reported in this region [e.g., *Holligan et al.*, 2010; *Poulton et al.*, 2013; *Balch et al.*, 2004].

Our observations of coccolithophore bloom duration may appear excessive when compared to other estimates (e.g., ~3 weeks in the North Atlantic [*Holligan et al.*, 1993a]). However, bloom duration in this analysis is based on the period that PIC concentration remains above the predetermined start and end bloom thresholds (e.g., Figure 2), which, it should be noted, are lower than the PIC concentrations typically associated with blooms as previously defined (e.g., >1000 cells mL^{-1} [*Tyrrell and Taylor*, 1996]). Given that detached coccoliths may remain visible from space after the organic cell population has begun to decline [*Tyrrell and Merico*, 2004], our estimates of bloom duration are potentially in excess of those determined from coccolithophore cell biomass and therefore most likely represent the upper bounds of how long a bloom lasts. The relatively low range in interannual variability observed in bloom duration (8–32 days) suggests that shifts in start date are matched by similar shifts in end date.

The North Atlantic exhibits the least interannual variability in start date and peak date over the 10 year period and has a latitudinal progression in start date that is similar to that observed in chlorophyll data [*Henson et al.*, 2009]. This suggests perhaps that the environmental conditions that influence the initiation of the noncalcifying phytoplankton bloom in this region may also exert a similar control on the initiation of the coccolithophore bloom. The low interannual variability observed in the phenological indices at extreme high latitudes results from the reduced satellite coverage that is common in these regions, while the higher levels of interannual variability noted in the equatorial regions and edges of the subtropical gyres are most likely caused by our algorithm having difficulty in isolating a definitive annual peak in data that have a low signal-to-noise ratio. In addition, high variability observed in some coastal regions may be due to the influence that resuspended material can have on PIC retrievals [*Broerse et al.*, 2003; *Weeks et al.*, 2004; *Daniels et al.*, 2012]. Our estimates of interannual variability are therefore likely to be most reliable in the midlatitudes (~40°–60°).

4.2. Succession or Coexistence

Our comparative analysis of the timing of PIC and chlorophyll peaks indicates that blooms of coccolithophores can occur at the same time as blooms of other noncalcifying phytoplankton over large areas of the open ocean.

This supports in situ observations of coccolithophores coexisting with other phytoplankton taxa [*Holligan et al.*, 1993a; *Poulton et al.*, 2013; *Balch et al.*, 2014] and the findings of *Barber and Hiscock* [2006] which suggest that one taxon can coexist with, rather than replace, another taxon through differences in biomass accumulation rates (net population growth rates), while actual competition between the two populations is kept in check through variability in nutrient uptake rates and shifts in the dominant grazers and the overall food web structure. Where coccolithophores coexist with other phytoplankton taxa (in our analysis peaks in concentration occur within ±16 days of each other), subtle physiological and ecological differences may ensure sufficient ecological diversity to overcome competitive exclusion [*Hardin*, 1960] and allow coexistence.

However, in those areas where there is a greater difference in timing of the chlorophyll and PIC peaks (in our analysis > 24 days), the observed pattern appears to support *Margalef*'s [1978] suggestion that environmental changes promote the proliferation of one taxa at the expense of another. Areas that display these attributes of succession might be expected to be regions where significant shifts in environmental conditions lead to equally significant shifts in phytoplankton populations. Although the mean chlorophyll concentrations from the succession and coexistence regions are not statistically different (two-sample, two-tailed t test; $p > 0.1$), there is a statistically significant difference in the spatial variability in data from the two regions (two-sample f test; $p < 0.05$). The spatial variability in chlorophyll data in areas displaying succession characteristics is noted to be greater (standard deviation $= 5.7 \, \mathrm{mg \, m^{-3}}$) than in regions that exhibit coexistence (standard deviation $= 2.2 \, \mathrm{mg \, m^{-3}}$). This suggests that regions of succession are more likely to be associated with higher spatial variability in chlorophyll concentration, which in turn might suggest that these regions may be associated with blooms of larger microphytoplankton ($> 20 \, \mu m$) such as diatoms, which can outcompete other taxa early in the growing season.

In areas that exhibit succession characteristics, early blooms of microphytoplankton (e.g., diatoms) will draw down nutrients such as silicic acid and iron to the point where these larger taxa will eventually decline. This then opens up an ecological niche for smaller phytoplankton ($< 20 \, \mu m$), such as coccolithophores, that are better adapted for survival in low silicic acid [*Holligan et al.*, 1983; *Townsend et al.*, 1994] and low iron environments [*Brand et al.*, 1983; *Muggli and Harrison*, 1997]. In areas that have the characteristics of coexistence, the low variability in chlorophyll concentration suggests that perhaps through differing physiological and/or ecological pressures, a bloom of larger phytoplankton may fail to establish to the same extent as that found in the succession environments. This inability to establish a bloom dominated by microplankton with higher chlorophyll content, possibly because of the limited availability of specific resources (e.g., silicic acid and iron), may then enable coccolithophores, with their lack or lower requirement for such resources [*Brand et al.*, 1983; *Muggli and Harrison*, 1997], to coexist with the other small phytoplankton within the bloom. Interestingly, it has also been previously suggested that in iron-limited regions, *E. huxleyi* may make a greater contribution to the total phytoplankton population because of its lower iron requirement [*Holligan et al.*, 2010].

If dissolved iron does indeed exert some influence over whether microphytoplankton taxa such as diatoms are able to establish early, dominant blooms that may drive succession, then it might be expected that those regions where succession is typical would be associated with higher iron concentrations than those regions where coexistence is more common. *Moore et al.* [2013] identified dissolved iron as being the primary limiting nutrient in areas where we have identified characteristics of coexistence, including the Southern Ocean and parts of the North Pacific and North Atlantic. In addition, the areas we have identified as regions of succession and coexistence broadly correspond with regions of high and low iron availability recently diagnosed from a global model of upper ocean dissolved iron concentration [*Misumi et al.*, 2014]. It was found that pixels with succession characteristics were associated with significantly higher dissolved iron concentrations than those pixels with the characteristics of coexistence (two-sample t test; $p < 0.05$).

Previous work has suggested that fast-growing, larger microphytoplankton such as diatoms are likely to dominate phytoplankton community structure in eutrophic environments with sufficiently high concentrations of dissolved silicic acid and that coccolithophores may only be able to establish dominance once this population declines [*Tyrrell and Merico*, 2004]. This has led to the suggestion that coccolithophore blooms might be associated with the low levels of silicic acid found after diatom blooms [e.g., *Townsend et al.*, 1994; *Tyrrell and Merico*, 2004; *Poulton et al.*, 2013; *Balch et al.*, 2014]. While the underlying concept of

competition between diatoms and coccolithophores may be significant in determining the makeup of community structure within a bloom, it is perhaps not solely silicic acid concentration that determines the outcome. Colimitation with iron may also dictate whether small phytoplankton, such as coccolithophores, have a competitive advantage [*Brzezinski et al.*, 2011].

Our conclusions regarding the coexistence and succession of phytoplankton populations rely on the assumptions that (a) changes in PIC concentration are globally representative of changes in coccolithophore biomass and (b) early changes in chlorophyll concentration are dominated by changes in the biomass of microphytoplankton that have a higher chlorophyll content than coccolithophores, such as diatoms. We recognize that this may not always be the case, particularly in regions where other processes may influence retrievals of PIC such as the Bering Sea [*Broerse et al.*, 2003], off the Namibian coast [*Weeks et al.*, 2004] and the Bay of Biscay [*Daniels et al.*, 2012], or in areas where environmental conditions may be unfavorable for the development of populations of large phytoplankton and thus where the chlorophyll signal may represent an underlying population of smaller phytoplankton.

5. Conclusions

Our analysis of remotely sensed PIC concentration has generated global maps of key phenological characteristics, such as start date, peak date, and duration of coccolithophore blooms. These data, in conjunction with chlorophyll phenology data, have enabled us to compare the timings of coccolithophore blooms with those of other noncalcifying phytoplankton taxa in the global ocean. We find evidence to support the canonical view of a succession of phytoplankton in some areas, particularly shelf regions, some areas of upwelling, and the high latitude North Atlantic. There is, however, strong evidence of coexistence of phytoplankton populations across a large proportion of the open ocean. Our data strongly contradict the hypothesis that phytoplankton succession is a universal feature of seasonal dynamics, showing instead that coexistence is typical in many areas.

References

Balch, W. M. (2004), Re-evaluation of the physiological ecology of coccolithophores, in *Coccolithophores: From Molecular Processes to Global Impact*, edited by H.-R. Thiersten and J. R. Young, Springer, Berlin.

Balch, W. M., P. M. Holligan, S. G. Ackleson, and K. J. Voss (1991), Biological and optical properties of mesoscale coccolithophore blooms in the Gulf of Maine, *Limnol. Oceanogr.*, *36*(4), 629–643.

Balch, W. M., K. A. Kilpatrick, P. M. Holligan, D. S. Harbour, and E. Fernandez (1996), The 1991 coccolithophore bloom in the central North Atlantic: 2. Relating optics to coccolith concentration, *Limnol. Oceanogr.*, *41*, 1684–1696.

Balch, W. M., H. R. Gordon, B. C. Bowler, D. T. Drapeau, and E. S. Booth (2005), Calcium carbonate measurements in the surface global ocean based on Moderate-Resolution Imaging Spectroradiometer data, *J. Geophys. Res.*, *110*, C07001, doi:10.1029/2004JC002560.

Balch, W. M., A. J. Plueddeman, B. C. Bowler, and D. T. Drapeau (2009), Chalk-Ex—Fate of $CaCO_3$ particles in the mixed layer: Evolution of patch optical properties, *J. Geophys. Res.*, *114*, C07020, doi:10.1029/2008JC004902.

Balch, W. M., D. T. Drapeau, B. C. Bowler, E. Lyczskowski, E. S. Booth, and D. Alley (2011), The contribution of coccolithophores to the optical and inorganic carbon budget during the Southern Ocean Gas Exchange Experiment: New evidence in support of the "Great Calcite Belt" hypothesis, *J. Geophys. Res.*, *116*, C00F06, doi:10.1029/2011JC006941.

Balch, W. M., D. T. Drapeau, B. C. Bowler, E. R. Lyczkowski, L. C. Lubelczyk, S. C. Painter, and A. J. Poulton (2014), Surface biological, chemical, and optical properties of the Patagonian Shelf coccolithophore bloom, the brightest waters of the Great Calcite Belt, *Limnol. Oceanogr.*, *59*(5), 1715–1732, doi:10.4319/lo.2014.59.5.1715.

Barber, R. T., and M. R. Hiscock (2006), A rising tide lifts all phytoplankton: Growth response of other phytoplankton taxa in diatom-dominated blooms, *Global Biogeochem. Cycles*, *20*, GB4S03, doi:10.1029/2006GB002726.

Brand, L. E., W. G. Sunda, and R. R. L. Guillard (1983), Limitation of marine phytoplankton reproductive rates by zinc, manganese, and iron, *Limnol. Oceanogr.*, *28*(6), 1182–1198.

Brody, S. R., M. S. Lozier, and J. P. Dunne (2013), A comparison of methods to determine phytoplankton bloom initiation, *J. Geophys. Res. Ocean.*, *118*, 2345–2357, doi:10.1002/jgrc.20167.

Broecker, W., and E. Clark (2009), Ratio of coccolith $CaCO_3$ to foraminifera $CaCO_3$ in late Holocene deep sea sediments, *Paleoceanography*, *24*, PA3205, doi:10.1029/2009PA001731.

Broerse, A. T. C., T. Tyrrell, J. R. Young, A. J. Poulton, A. Merico, W. M. Balch, and P. I. Miller (2003), The cause of bright waters in the Bering Sea in winter, *Cont. Shelf Res.*, *23*(16), 1579–1596, doi:10.1016/j.csr.2003.07.001.

Brown, C. W., and J. A. Yoder (1994), Coccolithophorid blooms in the global ocean, *J. Geophys. Res.*, *99*(C4), 7467–7482, doi:10.1029/93JC02156.

Brzezinski, M. A., et al. (2011), Co-limitation of diatoms by iron and silicic acid in the equatorial Pacific, *Deep Sea Res. Part II*, *58*(3–4), 493–511, doi:10.1016/j.dsr2.2010.08.005.

Claustre, H., and S. Maritorena (2003), The many shades of ocean blue, *Science*, *302*(5650), 1514–1515.

Cole, H., S. Henson, A. Martin, and A. Yool (2012), Mind the gap: The impact of missing data on the calculation of phytoplankton phenology metrics, *J. Geophys. Res.*, *117*, C08030, doi:10.1029/2012JC008249.

Daniels, C. J., T. Tyrrell, A. J. Poulton, and L. Pettit (2012), The influence of lithogenic material on particulate inorganic carbon measurements of coccolithophores in the Bay of Biscay, *Limnol. Oceanogr.*, *57*(1), 145–153.

Daniels, C. J., R. M. Sheward, and A. J. Poulton (2014), Biogeochemical implications of comparative growth rates of *Emiliania huxleyi* and *Coccolithus* species, *Biogeosciences*, *11*(23), 6915–6925, doi:10.5194/bg-11-6915-201.

Doney, S. C., V. J. Fabry, R. A. Feely, and J. Kleypas (2009), Ocean acidification: The other CO_2 problem, *Ann. Rev. Mar. Sci.*, *1*, 169–192.

González Taboada, F., and R. Anadón (2014), Seasonality of North Atlantic phytoplankton from space: Impact of environmental forcing on a changing phenology (1998–2012), *Global Change Biol.*, *20*(3), 698–712, doi:10.1111/gcb.12352.

Gordon, H. R., O. B. Brown, R. H. Evans, J. W. Brown, R. C. Smith, K. S. Baker, and D. K. Clark (1988), A semianalytic radiance model of ocean color, *J. Geophys. Res.*, *93*(D9), 10,909–10,924, doi:10.1029/JD093iD09p10909.

Gordon, H. R., G. C. Boynton, W. M. Balch, S. B. Groom, D. S. Harbour, and T. J. Smyth (2001), Retrieval of coccolithophore calcite concentration from SeaWiFS imagery, *Geophys. Res. Lett.*, *28*(8), 1587–1590, doi:10.1029/2000GL012025.

Hardin, G. (1960), The competitive exclusion principle, *Science*, *131*(3409), 1292–1297.

Harlay, J., et al. (2010), Biogeochemical study of a coccolithophore bloom in the northern Bay of Biscay (NE Atlantic Ocean) in June 2004, *Prog. Oceanogr.*, *86*(3–4), 317–336, doi:10.1016/j.pocean.2010.04.029.

Henson, S. A., J. P. Dunne, and J. L. Sarmiento (2009), Decadal variability in North Atlantic phytoplankton blooms, *J. Geophys. Res.*, *114*, C04013, doi:10.1029/2008JC005139.

Henson, S. A., R. Sanders, and E. Madsen (2012), Global patterns in efficiency of particulate organic carbon export and transfer to the deep ocean, *Global Biogeochem. Cycles*, *26*, GB1028, doi:10.1029/2011GB004099.

Holligan, P. M., M. Viollier, D. S. Harbour, P. Camus, and M. Champagne-Phillipe (1983), Satellite and ship studies of coccolithophore production along a continental shelf edge, *Nature*, *304*, 339–342.

Holligan, P. M., et al. (1993a), A biogeochemical study of the coccolithophore, Emiliania huxleyi, in the North Atlantic, *Global Biogeochem. Cycles*, *7*(4), 879–900, doi:10.1029/93GB01731.

Holligan, P. M., S. Groom, and D. Harbour (1993b), What controls the distribution of the coccolithophore, Emiliania huxleyi, in the North Sea?, *Fish. Oceanogr.*, *2*(3–4), 175–183, doi:10.1111/j.1365-2419.1993.tb00133.x.

Holligan, P. M., A. Charalampopoulou, and R. Hutson (2010), Seasonal distributions of the coccolithophore, Emiliania huxleyi, and of particulate inorganic carbon in surface waters of the Scotia Sea, *J. Mar. Syst.*, *82*(4), 195–205, doi:10.1016/j.jmarsys.2010.05.007.

Hovland, E. K., H. M. Dierssen, A. S. Ferreira, and G. Johnsen (2013), Dynamics regulating major trends in Barents Sea temperatures and subsequent effect on remotely sensed particulate inorganic carbon, *Mar. Ecol. Prog. Ser.*, *484*, 17–32, doi:10.3354/meps10277.

Iglesias-Rodríguez, M. D., C. W. Brown, S. C. Doney, J. Kleypas, D. Kolber, Z. Kolber, P. K. Hayes, and P. G. Falkowski (2002), Representing key phytoplankton functional groups in ocean carbon cycle models: Coccolithophorids, *Global Biogeochem. Cycles*, *16*(4), 1100, doi:10.1029/2001GB001454.

Ji, R., M. Edwards, D. L. Mackas, J. A. Runge, and A. C. Thomas (2010), Marine plankton phenology and life history in a changing climate: Current research and future directions, *J. Plankton Res.*, *32*, 1355–1368.

Klaas, C., and D. E. Archer (2002), Association of sinking organic matter with various types of mineral ballast in the deep sea: Implications for the rain ratio, *Global Biogeochem. Cycles*, *16*(4), 1116, doi:10.1029/2001GB001765.

Margalef, R. (1978), Life-forms of phytoplankton as survival alternatives in an unstable environment, *Oceanol. Acta*, *1*(4), 493–509.

Miller, C. B. (2004), The spring phytoplankton bloom, in *Biological Oceanography*, pp. 1–19, Blackwell Publishing, Oxford.

Milliman, J. D. (1993), Production and accumulation of calcium carbonate in the ocean: Budget of a non-steady state, *Global Biogeochem. Cycles*, *7*(4), 927–957, doi:10.1029/93GB02524.

Misumi, K., K. Lindsay, J. K. Moore, S. C. Doney, F. O. Bryan, D. Tsumune, and Y. Yoshida (2014), The iron budget in ocean surface waters in the 20th and 21st centuries: Projections by the Community Earth System Model version 1, *Biogeosciences*, *11*(1), 33–55, doi:10.5194/bg-11-33-2014.

Moore, C. M., et al. (2013), Processes and patterns of oceanic nutrient limitation, *Nat. Geosci.*, *6*(9), 701–710, doi:10.1038/ngeo1765.

Morel, A., and L. Prieur (1977), Analysis of variations in ocean color, *Limnol. Oceanogr.*, *22*(4), 709–722, doi:10.4319/lo.1977.22.4.0709.

Muggli, D. L., and P. J. Harrison (1997), Effects of iron on two oceanic phytoplankters grown in natural NE subarctic pacific seawater with no artificial chelators present, *J. Exp. Mar. Biol. Ecol.*, *212*, 225–237.

Paasche, E. (2002), A review of the coccolithophorid Emilinia huxleyi (Prymnesiophyceae), with particular reference to growth, formation, and calcification-photosynthesis interactions, *Phycologia*, *40*(6), 503–529.

Poulton, A. J., T. R. Adey, W. M. Balch, and P. M. Holligan (2007), Relating coccolithophore calcification rates to phytoplankton community dynamics: Regional differences and implications for carbon export, *Deep Sea Res., Part II*, *54*, 538–557.

Poulton, A. J., A. Charalampopoulou, J. R. Young, G. A. Tarran, M. I. Lucas, and G. D. Quarterly (2010), Coccolithophore dynamics in non-bloom conditions during late summer in the central Iceland Basin (July–August 2007), *Limnol. Oceanogr.*, *55*(4), 1601–1613.

Poulton, A. J., S. C. Painter, J. R. Young, N. R. Bates, B. Bowler, D. Drapeau, E. Lyczsckowski, and W. M. Balch (2013), The 2008 Emiliania huxleyi bloom along the Patagonian Shelf: Ecology, biogeochemistry, and cellular calcification, *Global Biogeochem. Cycles*, *27*, 1023–1033, doi:10.1002/2013GB004641.

Racault, M.-F., C. Le Quere, E. Buitenhuis, S. Sathyendranath, and T. Platt (2012), Phytoplankton phenology in the global ocean, *Ecol. Indic.*, *14*(1), 152–163.

Racault, M.-F., T. Platt, S. Sathyendranath, E. Agrbas, V. Martinez Vicente, and R. Brewin (2014), Plankton indicators and ocean observing systems: Support to the marine ecosystem state assessment, *J. Plankton Res.*, *36*(3), 621–629, doi:10.1093/plankt/fbu016.

Raitsos, D. E., S. J. Lavender, Y. Pradhan, T. Tyrrell, P. C. Reid, and M. Edwards (2006), Coccolithophore bloom size variation in response to the regional environment of the subarctic North Atlantic, *Limnol. Oceanogr.*, *51*(5), 2122–2130.

Schiebel, R., U. Brupbacher, S. Schmidtko, G. Nausch, J. J. Waniek, and H.-R. Thiersten (2011), Spring coccolithophore production and dispersion in the temperate eastern North Atlantic Ocean, *J. Geophys. Res.*, *116*, C08030, doi:10.1029/2010JC006841.

Shutler, J. D., M. G. Grant, P. I. Miller, E. Rushton, and K. Anderson (2010), Coccolithophore bloom detection in the northeast Atlantic using SeaWiFS: Algorithm description, application and sensitivity analysis, *Remote Sens. Environ.*, *114*(5), 1008–1016, doi:10.1016/j.rse.2009.12.024.

Shutler, J. D., P. E. Land, C. W. Brown, H. S. Findlay, C. J. Donlon, M. Medland, R. Snooke, and J. C. Blackford (2013), Coccolithophore surface distributions in the North Atlantic and their modulation of the air-sea flux of CO_2 from 10 years of satellite Earth observation data, *Biogeosciences*, *10*, 2699–2709.

Siegel, D. A., S. C. Doney, and J. A. Yoder (2002), The North Atlantic spring bloom and Sverdrup's critical depth theory, *Science*, *296*(5568), 730–733.

Signorini, S. R., and C. R. McClain (2009), Environmental factors controlling the Barents Sea spring-summer phytoplankton blooms, *Geophys. Res. Lett.*, *36*, L10604, doi:10.1029/2009GL037695.

Signorini, S. R., V. M. T. Garcia, A. R. Piola, C. A. E. Garcia, M. M. Mata, and C. R. McClain (2006), Seasonal and interannual variability of calcite in the vicinity of the Patagonian shelf break (38°S–52°S), *Geophys. Res. Lett.*, *33*, L16610, doi:10.1029/2006GL026592.

Smayda, T. J. (1997), What is a bloom? A commentary, *Limnol. Oceanogr.*, *42*(5–2), 1132–1136.

Smyth, T. J., T. Tyrrell, and B. Tarrant (2004), Time series of coccolithophore activity in the Barents Sea, from twenty years of satellite imagery, *Geophys. Res. Lett.*, *31*, L11302, doi:10.1029/2004GL019735.

Smyth, T. J., I. Allen, A. Atkinson, J. T. Bruun, R. A. Harmer, R. D. Pingree, C. E. Widdicombe, and P. J. Somerfield (2014), Ocean net heat flux influences seasonal to interannual patterns of plankton abundance, *PLoS One*, *9*(2), doi:10.1371/journal.pone.0098709.

Taylor, J. R., and R. Ferrari (2011), Shutdown of turbulent convection as a new criterion for the onset of spring phytoplankton blooms, *Limnol. Oceanogr.*, *56*(6), 2293–2307, doi:10.4319/lo.2011.56.6.2293.

Townsend, D. W., M. D. Keller, P. M. Holligan, S. G. Ackleson, and W. M. Balch (1994), Blooms of coccolithophore Emiliania huxleyi with respect to the hydrography in the Gulf of Maine, *Cont. Shelf Res.*, *14*(9), 979–1000.

Tyrrell, T., and A. Merico (2004), Emiliania huxleyi: Bloom observations and the conditions that induce them, in *Coccolithophores: From Molecular Processes to Global Impact*, edited by H.-R. Thiersten and J. R. Young, pp. 75–97, Springer, Heidelberg.

Tyrrell, T., and A. H. Taylor (1996), A modelling study of Emiliania huxleyi in the NE Atlantic, *J. Mar. Syst.*, *9*, 83–112.

Weeks, S. J., B. Currie, A. Bakun, and K. R. Peard (2004), Hydrogen sulphide eruptions in the Atlantic Ocean off southern Africa: Implications of a new view based on SeaWiFS satellite imagery, *Deep Sea Res., Part I*, *51*(2), 153–172, doi:10.1016/j.dsr.2003.10.004.

Winter, A., R. W. Jordan, and P. H. Roth (1994), Biogeography of living coccolithophores in oceanic waters, in *Coccolithophores*, edited by A. Winter and W. G. Siesser, pp. 161–177, Cambridge Univ. Press, Cambridge.

Yoder, J. A., C. R. McClain, G. C. Feldman, and W. E. Esaias (1993), Annual cycles of phytoplankton chlorophyll concentrations in the global ocean: A satellite view, *Global Biogeochem. Cycles*, *7*(1), 181–193, doi:10.1029/93GB02358.

Young, J. R., A. J. Poulton, and T. Tyrrell (2014), Morphology of Emiliania huxleyi coccoliths on the northwestern European shelf—Is there an influence of carbonate chemistry?, *Biogeosciences*, *11*(17), 4771–4782, doi:10.5194/bg-11-4771-2014.

Zhai, L., T. Platt, C. Tang, S. Sathyendranath, and R. Herna (2011), Phytoplankton phenology on the Scotian Shelf, *ICES J. Mar. Sci.*, *68*, 781–791.